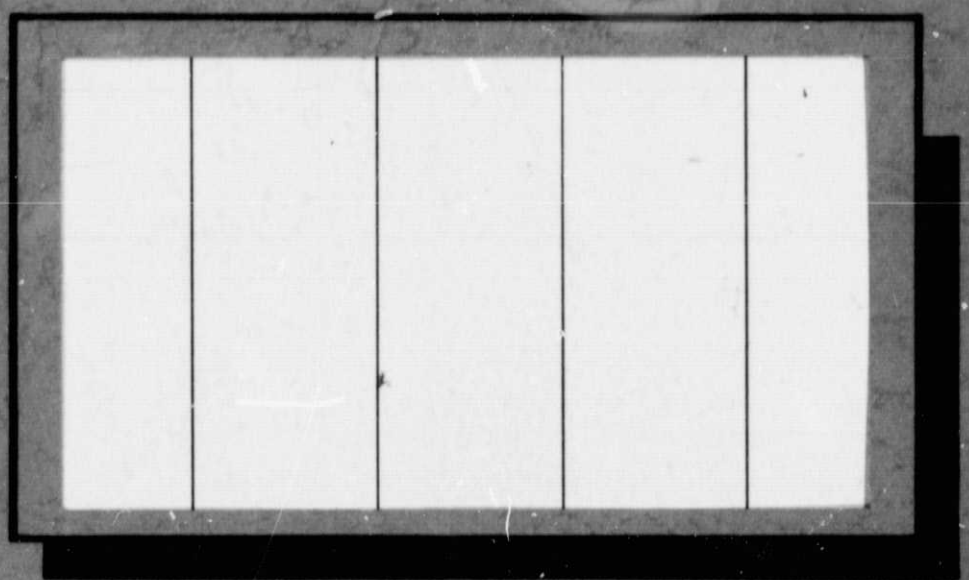

CENTER FOR SPACE RESEARCH
MASSACHUSETTS INSTITUTE OF TECHNOLOGY

SUBSTORMS ON MERCURY?

by

G. L. Siscoe, N. F. Ness[1], and C. M. Yeates[2]

July, 1974

Technical Report #CSR-TR-75-1

Department of Physics and Center for Space Research

Massachusetts Institute of Technology

Cambridge, Massachusetts 02139

[1] Goddard Space Flight Center, Greenbelt, Maryland 20771

[2] Jet Propulsion Laboratory, Pasadena, California 91109

ABSTRACT

The Mariner 10 encounter of Mercury provided data showing a strong interaction between the solar wind and the planet similar to a scaled-down version of that for the Earth's magnetosphere. Some of the features observed in the night-side Mercury magnetosphere suggest time-dependent processes occurring there. Interpreted as temporal events, these features bear striking resemblances to substorm phenomena in the Earth's magnetosphere.

INTRODUCTION

Instruments on the Mariner 10 spacecraft measured the particle and field environment of Mercury along a close, nightside encounter trajectory. The data provided a partial glimpse of an unexpected picture, which included a substantial magnetic field associated with the planet, deflected solar wind flow and related particle populations (Ogilvie et al., 1974; Ness et al., 1974; Simpson et al., 1974). The particles and fields showed large and complex correlated variations during the encounter period. Some of the features have familiar interpretations, such as a bow shock and a boundary, analogous to the magnetopause of Earth, separating the shocked solar wind (magnetosheath) plasma from plasma in the Mercury-associated magnetic field. (We use the designation Mercury-associated field rather than planetary field since it has not been shown that the data preclude a solar wind induced field). Inside the magnetopause-like boundary the variations were highly structured suggesting that if they represent spatial variations the particle and field configuration at Mercury must be very complicated. However, as is true for all single spacecraft missions, it is difficult to determine if a variation is spatial or temporal. The purpose of this note is to point out qualitative similarities between some of the variations in the Mercury encounter data and variations in the corresponding regions of the Earth's magnetosphere during substorms. Future measurements at Mercury might show that some of the correspondences suggested here have other explanations, but our purpose is to identify all possible correspondences.

REVIEW OF OBSERVATIONS

Figure 1 shows two projections of the Mariner 10 encounter trajectory: one as viewed from the north ecliptic pole and one as viewed from the sun. The numbers mark the locations of features in the data to be discussed below. Figure 2 shows combined data fields from the plasma (Ogilvie et al., 1974), magnetometer (Ness et al., 1974), and energetic particle (Simpson et al., 1974) experiments. As noted in these references, the data indicate a magnetic barrier deflecting the solar wind around the planet, with associated features familiar to the solar wind interaction with the Earth's magnetosphere: bow shock crossings at 1 and 9 (the outbound shock crossing is characterized by large fluctuations consistent with the existence of a pulsating shock as expected for the observed orientation of the solar wind field) and magnetopause crossings at 2 and 7; marked by sudden changes in the direction and magnitude of the field, by plasma density changes (low inside to high outside) and by changes in the >100 ev plasma electron fluxes (high inside to low outside). We consider now in more detail the data from inside the magnetosphere: the interval from 2 to 7.

The magnetospheric observations: features and/or events?

Looking first at the magnetic field, we see that after entering the magnetosphere at 2, the spacecraft observed the field oriented very nearly in the anti-solar direction ($\theta \simeq 0$, $\phi \simeq 180^{o}$). The field strength is initially about 45γ but increases in magnitude almost monotonically to $\sim 100\gamma$ at point 4. Throughout this increase, the field maintains its near anti-

solar orientation. The field then begins a period of rapid magnitude variations that include a large net decrease in the field. The fluctuations continue up to the outbound magnetopause crossing and beyond. Also beginning with the magnitude decrease at 4, the field direction changes to an essentially northward orientation ($70^{o} \leq \theta \leq 90^{o}$) that persist out to the magnetopause. The ϕ-component of the field also changes during this interval, but since the field is mainly perpendicular to the ϕ-plane, large changes in ϕ correspond to small changes in the vector orientation.

For both the inbound and outbound magnetopause crossings, the field magnitude is greater inside the magnetosphere than in the magnetosheath. The field increases from 30γ to 45γ inbound and decreases from 50γ to 20γ outbound. For pressure balance the ratio of plasma pressure to magnetic pressure must be less inside the magnetopause than outside, and this is consistent with the observed changes in the electron thermal pressure across the magnetopause.

We note here for later reference that the field in the magnetosheath just prior to the inbound magnetopause crossing has a northward component ($\theta \sim +30^{o}$) and just after the outbound crossing the magnetosheath field has a southward component ($\theta \sim -40^{o}$).

On entering the magnetosphere, the plasma electron data show a decrease in the total density to less than the pre-shock solar wind value. However, there is an increase in the flux of electrons which have energies greater than ~ 100 ev. (The density is determined primarily by electrons with energies less than ~ 100 ev because of spectral characteristics). Comparison of the density and pressure shows that the electron temperature is greater in the magnetosphere than in the magnetosheath. The density remains rela-

tively constant until 4 where it decreases and with some fluctuation becomes essentially zero until the outgoing magnetopause crossing. The interval of decreased density corresponds to the interval of decreased magnetic field and large magnetic fluctuations.

The energetic plasma electron fluxes increase on entering the magnetosphere. There is a further general rise in flux reaching a fairly flat maximum covering the interval 4 to the outbound magnetopause. Just prior to the flat maximum, there is a short interval of decreased flux which begins at 3. The plasma electrons within the magnetosphere have very different spectral parameters than solar wind or magnetosheath electrons and form a distinctive magnetospheric population.

The locations of the four main energetic particle events reported by Simpson et al. (1974) are also indicated. These are included as supporting evidence that the phenomena observed were temporal in nature. The onset of the first (event A), the smallest of the four, coincides closely with the decrease in the energetic plasma electron flux at 3. The second and third events (events B and C) occur in the interval of reduced magnetic field and large fluctuations. These are the largest of the energetic particle events. The fourth event (D) occurs when the spacecraft is in the outbound magnetosheath and appears to terminate at the bow shock.

THE MAGNETOSPHERE OF MERCURY

For the purpose of comparing the Mercury events with geomagnetic substorms, we assume the Mercury magnetosphere to be a scaled-down version of the Earth's magnetosphere. We then use the magnetospheric scaling relations to locate the corresponding Earth position of the Mariner 10 trajectory. For this, we need an estimate of the strength, location, and orientation of the Mercury magnetic dipole. Figure 1 shows that Mariner 10 entered the magnetosphere in the southern portion of the near-tail region and exited in the equatorial-terminator region. The field was directed away from the planet on entry and it was directed northward before exit. These are the same orientations observed in corresponding regions of the Earth's magnetosphere, and suggest a southward oriented planetary dipole. Fitting the locations of the shock and magnetopause crossings to Earth-type magnetosphere profiles gives a dipole strength in the range 4×10^{-4} to 9×10^{-4} that of Earth (Ness et al., 1974; Ogilvie et al., 1974), where the range results from the imprecision in identifying the exact locations of the boundary crossings in the data. A least squares fit to a harmonic decomposition of the "quiet field" portion of the encounter data (the interval from 2 to 4) has been performed (Ness et al.,1975). The planetary field was assumed to be a centered dipole and the external field was assumed to be well represented by harmonics up to degree 2. The resulting fit to the quiet interval was excellent (RMS = 0.95γ). The analysis gave a dipole strength of 5.1×10^{22} Gauss-cm^3 (6.4×10^{-4} that of Earth) with a vector direction 10° from the south ecliptic pole. The external field contribution was consistent with that expected from boundary and tail fields similar to those of Earth.

The distance scaling ratio is the ratio of the distances from the dipoles to the stagnation points for Earth and Mercury, given by

$$R_m^*/R_e^* = (M_M/M_E)^{1/3} \ (P_E/P_M)^{1/6}$$

where M designates magnetic moment and P designates the solar wind stagnation pressure. The stagnation pressure just prior to Mercury encounter was measured to be the equivalent of the pressure of a 166 $\pm$ 25γ magnetic field (Ogilvie et al., 1974). For Earth a typical stagnation pressure is 53γ for which $R_E^* = 11\ R_E$ (Fairfield, 1971). Thus, with $M_m = 6.4 \times 10^{-4} M_E$, we find

$$R_m^* = (1.7 \pm 0.1) R_m$$

Thus the stagnation point lies between 0.6 R_m and 0.8 R_m above the sub-solar surface of the planet. To allow direct comparison with the previous publications on the Mariner 10 data we adopt the value $R_m^* = 1.6 R_m$. (Also we use $1R_e$ = 6370 km and $1R_m$ = 2439 km.) The above scaling relation can be re-expressed as $1R_m$ distance in the Mercury magnetosphere, corresponds to $6.9R_E$ distance in the Earth magnetosphere. Translation of the Mariner 10 trajectory to the Earth's magnetosphere, then, gives magnetosphere entry at $X_E = -12.7\ R_E$ and magnetosphere exit at $X_E = -5.0\ R_E$. The corresponding distance where the magnetic field changes from away from the planet to northward (4 in Figure 1) is $X_E = -8.0\ R_E$. This region in the Earth's magnetosphere is near the nightside cusp which is the transition region between a dipole field orientation at closer distances to a tail-like field orientation at greater distances.

In the z-direction, Figure 1 shows that the spacecraft entered the tail south of any expected neutral sheet, but possibly within a plasma sheet if its geometry is similar to Earth's. Relative to the dipole axis shown in Figure 1, the trajectory approaches the neutral sheet position, and also enters more deeply into the plasma sheet region. Around point 4, it moves into the magnetosphere proper, that is, sunward of the region dominated by the tail current.

REVIEW OF SUBSTORM PHENOMENA IN THE EARTH MAGNETOSPHERE

Although full theoretical understanding of the substorm phenomena does not exist, there is a fairly complete phenomenological description. We give a partial list of substorm phenomena, relevant to the Mercury observations (see the review by Russell and McPherron, 1973, for further details and references). The location of Mariner 10 entry into the Mercury magnetosphere corresponds to the plasmasheet or the lobe just below the plasmasheet in the Earth magnetotail. Near the onset of substorms the plasmasheet thins to a narrow region near the magnetic neutral sheet. Thus, except for spacecraft located very near the neutral sheet, plasmasheet electron fluxes decrease near the onset of a substorm. The magnetic field strength increases but the orientation remains tail-like, i.e., away from (Southern hemisphere) or toward (Northern hemisphere) the planet. Electron fluxes return with greater intensities near the end of the substorm.

In the cusp region ($X = -8\ R_E$ to $-11\ R_E$), the magnetic field shows the largest change in response to substorms. Here the occurrence of a substorm causes the field strength to decrease and to change from tail-like to dipole-like (Fairfield and Ness, 1970; McPherron, 1972). Thus, in the cusp region and south of the dipole equatorial plane, the field orientation changes from pointing away from the planet to pointing northward during a substorm. Electron fluxes in this region increase during substorms (Frank, 1971).

Energetic electron events (electrons with energies > 30 KeV) in the tail and magnetosheath and outside the bow shock have been reported by Anderson (1965, 1968) and Anderson et al. (1965). Subsequent analysis and correlations (Murayama, 1966; Anderson and Ness, 1966; Meng and Anderson, 1971;

Hones et al., 1972) indicate that at least some of these events are associated with substorm thinning and thickening of the plasma-sheet. They characteristically occur as short isolated bursts with a rapid rise in flux (several minutes or less) and a longer decay. They appear both in the tail and dawnside magnetosheath, and upstream from the bow shock.

Substorms at Earth have a typical duration of ½ to 1 hour. The rate of occurrence of large substorms is known to depend on the orientation of the solar wind magnetic field. If the solar wind field has a northward component (i.e., antiparallel to the dipole orientation) the occurrence rate is low and the magnetosphere and tail are characterized as being quiet. If the solar wind field has a substantial southward component (i.e., parallel to the dipole orientation) the occurrence rate is high, of the order of 1 per hour, and the magnetosphere and tail are characterized as disturbed. Scaling of the characteristic substorm times to the Mercury magnetosphere is considered in the next section.

POSSIBLE SUBSTORMS AT MERCURY

In drawing analogies between the events observed by Mariner 10 at Mercury and substorm phenomena at Earth, we should not expect a perfect or detailed correspondence, since the scaling relations for substorm processes are only approximate and in some cases (for example the energetic particle events) are not well known. The sizes of the planets do not scale as the magnetospheric size, and the planet Mercury occupies a much larger portion of its magnetosphere. Also the ionospheres do not scale as the magnetospheres. Mercury apparently has a negligible ionosphere (Howard et al., 1974; Ogilvie et al., 1974). Thus, ionospheric effects which are thought to be important in substorm processes at Earth could be absent at Mercury. Nevertheless we feel that a possible correspondence between the observed Mercury events and terrestrial substorms is quite likely. To demonstrate the correspondence, we interpret the data shown in Figure 1 as if they were obtained on the corresponding scaled trajectory in the Earth magnetosphere.

The spacecraft entered the near-tail, evening side, south latitude magnetosphere at 2. Before entry, the magnetosheath field had a northward component, and the tail field after entry was radially away from the planet and relatively quiet. The presence of plasma electrons indicates that the spacecraft was in the plasma sheet. At 3 the energetic plasma electrons in the plasma sheet decreased, the field increased and a small energetic particle event, A, occurred. This could signal the onset of convection with thinning of the plasmasheet, that is, the so-called growth phase of a substorm, although in the Earth's magnetosphere energetic particle events have not been identified with the growth phase of a substorm. At 4 the

spacecraft was in the cusp region and a substorm occurred with a consequent decrease in field strength and change in field orientation from tail-like to dipole-like. The interval of magnetic disturbance began. Energetic plasma electron fluxes increased to their highest values. An energetic particle event, B, with a fast-rise, slow-decay profile is associated with this event. Event B begins about one minute later than the substorm onset. The particles may have been created elsewhere and drifted to the location of the spacecraft. We have not attempted to scale such a process for comparison with the Earth's situation. Subsequently, as the spacecraft passed through the morning magnetosphere, further disturbances occurred beginning at 5 indicated by the large field strength variations and another energetic particle event, C, at 6. The spacecraft exited the magnetosphere into the dawnside magnetosheath at 7 and observed a southward component to the magnetosheath field. The occurrence of another substorm is suggested by the energetic particle event at 8 while the magnetosheath field was still southward. The magnetosheath field then turned to northward and no subsequent particle events were observed.

A solid line drawn mentally as an envelope over the peaks of F in Figure 2 would illustrate our interpretation of the data. The envelope represents the field strength in the absence of substorms and the pronounced negative deviations from the envelope are substorm effects.

We postulate that the magnetosheath field changed from northward to southward while the spacecraft was deep within the magnetosphere. This is consistent with the onset of convection and substorms when the spacecraft was approximately half way through the magnetosphere. It is also consistent with the magnetosheath field being northward just prior to entry and southward just after exit from the magnetosphere. Since the magnetosphere is in

contact with the magnetosheath field, these observations are more directly indiciative of the state of merging than are solar wind measurements. However, since the entire magnetosphere passage took only 17 minutes, we must determine if the time scale for substorms at Mercury is short compared to 17 minutes. The relevant scale is the convection time T_c defined as the time to cycle the magnetic flux in the tail F_T under the action of the electric potential ϕ_c across the magnetosphere: $T_c = F_T/\phi_c$. With $F_T = 2\pi R_m{}^{*2} B_T$ and $\phi_c = V_{sw} B_{sw} R_m{}^*$, where B_T = tail field strength and subscript sw denotes solar wind parameters, we have $T_c = 2\pi B_T R_m{}^*/B_{sw} V_{sw}$. For Earth $B_T \simeq 20\gamma$, $B_{sw} \simeq 5\gamma$, $V_{sw} \simeq 400$ km/sec and $R_m{}^* \simeq 10\ R_E$ are the typical values giving $(T_c)_E \simeq$ 1 hr in agreement with the observed time scale for substorms. At the time of Mercury encounter $V_{sw} \simeq 600$ km/sec, $B_T \simeq 40\gamma$, $B_{sw} \simeq 20\gamma$, and $R_m{}^* \simeq 1.6\ R_m$, giving $(T_c)_M \simeq 1.2$ minutes. This must be regarded as a factor of two estimate since no distinction is made between the lobe and plasmasheet field and only the component of the B_{sw} field in the direction of the dipole axis should enter. However, the same approximations were made in estimating T_c for the earth, so the ratio of the two time scales is more accurate than the absolute values. Thus, the occurrence of several substorms during the Mariner 10 encounter after the solar wind field turned southward is consistent with the Mercury substorm time scale.

Another way of expressing the scaling is that $(T_c)_E \simeq 50\ (T_c)_M$. Thus, 17 minutes at Mercury is equivalent to approximately 14 hours at Earth. Over a long time average, substorms at Earth occur approximately once every 3 hours. Thus on average a 14-hour pass through the Earth magnetosphere would yield approximately four substorms. Although the fluctuations around the average are large, the observed correspondence of substorm frequency shows that this interpretation is reasonable even though the encounter interval at Mercury was short.

SUBSTORM ENERGIZATION

It is of interest to extend the substorm analogy to consider the rate of energization of the Mercury magnetosphere during substorms. On the basis of our present understanding of substorm energization at Earth, the energization rate is given by the Poynting flux of energy into the tail along a length approximately equal to one magnetospheric scale length (Kennel, 1973; Siscoe and Crooker, 1974; Siscoe, 1974). This gives the input power $W = R_M^* \phi B_T/\mu_o$. The ratio of power at Mercury to Earth is then $W_M/W_E = (R_M^*/R_E^*)\ (\phi_M/\phi_E)(B_{TM}/B_{TE}) \sim 10^{-2}$. Estimates of the substorm input power at Earth fall in the range 10^{11} to 10^{12} watts. Thus, for Mercury we estimate $W_M \sim 10^9$ to 10^{10} watts. Using a substorm time scale of 2 minutes, we find a total energy input per substorm in the range 10^{11} to 10^{12} joules.

An estimate of the magnetic disturbance resulting from the energization can be made by equating the total energy to the interaction energy with the Mercury dipole (Carovillano and Siscoe, 1973): Energy $\sim B_{DIST}\, M_M$. This gives a range between 3γ and 30γ. However, large fluctuations around the average disturbance field should be expected because of the different scaling of energy and field. Since ϕ scales as R*, and T_c scales as R*, the total energy per substorm scales as $(R^*)^2$. Also the magnetosphere volume scales as $(R^*)^3$. Thus, the disturbance energy density at Mercury is the same as at Earth. However, the self energy density of the Mercury field in the magnetosphere scales as $M \cdot B_{surface} \cdot (R^*)^{-3} \sim 10^{-2}$ that of the Earth magnetic field self energy density. Thus, we expect the amplitude of substorm disturbance variations at Mercury to be larger than at Earth relative to the main field. This is consistent with the large relative disturbance in the Mercury magnetosphere after event 4.

COMMENTS

We have suggested an interpretation of some plasma-field events at Mercury in terms of substorms, especially those from 3 to 7. The substorm analogy is a specific example of a time dependent process that agrees fairly well with the observations, although alternative time dependent processes are possible. For example, if the Mercury magnetic field is induced by the solar wind, time dependent changes should occur whenever the solar wind field changes since the inducing electric field then changes. This substorm model would then imply that a consideration of the characteristic time scales of the induction mechanism would lead to values >> 1.2 minutes.

Verification or rejection of the substorm interpretation and the nature of the planet-associated magnetic field will require more observations at Mercury. The Mariner 10 observations show that there is a good possibility that Mercury offers an opportunity to study a scaled-down version of a magnetosphere devoid of an ionosphere. Mercury could be more useful than Jupiter in testing our understanding of magnetospheric dynamics since for Jupiter centrifugal forces play a dominant role and the dynamics are not directly comparable to Earth. However, the probable lack of a plasmasphere and an appreciable ionosphere also make Mercury not directly comparable to Earth, but this gives an opportunity to determine the importance of the ionosphere in magnetospheric dynamics. The substorm interpretation given here suggests that the ionosphere may not be very important in controlling at least the spasmodic nature of substorm occurrence.

ACKNOWLEDGEMENTS

This work was supported in part by the National Aeronautics and Space Administration under grants NGL 22-009-015 and NAS 5-9078 (M.I.T.). We thank the other members of the plasma science and magnetometer teams on Mariner 10, K. W. Behannon, R. P. Lepping, W. C. Whang, K. W. Ogilvie, J. D. Scudder, R. E. Hartle, H. S. Bridge, A. J. Lazarus, J. R. Asbridge, and S. J. Bame, for their important contributions to the overall experiment.

REFERENCES

Anderson, K. A., Energetic electron fluxes in the tail of the geomagnetic field, J. Geophys. Res., 70, 4741, 1965.

Anderson, K.A., and N.F. Ness, Correlation of magnetic fields and energetic electrons on the IMP 1 satellite, J. Geophys. Res., 71, 3705, 1966.

Anderson, K. A., H. K. Harris, and R. J. Paoli, Energetic electron fluxes in and beyond the Earth's outer magnetosphere, J. Geophys. Res., 70, 1039, 1965.

Anderson, K.A., Energetic electrons of terrestrial origin upstream in the solar wind, J. Geophysical Res., 73, 2387, 1968.

Carovillano, R. L., and G. L. Siscoe, Energy and momentum theorems in magnetospheric processes, Rev. Geophys. Space Phys., 11, 289, 1973.

Fairfield, D. H., and N. F. Ness, Configuration of the geomagnetic tail during substorms, J. Geophys. Res., 75, 7032, 1970.

Fairfield, D.H., Average and unusual location of the Earth's magnetopause and bow shock, J. Geophys. Res., 76, 6700, 1971.

Frank, L. A., Relationship of the plasma sheet, ring current, trapping boundary, and plasmapause near the magnetic equator and local midnight, J. Geophys. Res., 76, 2265, 1971.

Hones, E.W., Jr., S.-I. Akasofu, S.J. Bame, and S, Singer, Outflow of plasma from the magnetotail into the magnetosheath, J. Geophys. Res., 77, 6688, 1972.

Howard, H.T., G.L. Tyler, P.B. Esposito, J.D. Anderson, R.D. Reasenberg, I.I. Shapiro, G. Fjeldbo, A.J. Kline, G.S. Levy, D.L. Brunn, R. Dickinson, R.E. Edelson, W.L. Martin, R.B. Postal, B. Seidel, T.T. Sesplankis, D.L. Shirley, C.T. Stelgried, D.N. Sweetnam, G.E. Wood, and A.I. Zygielbaum, Mercury: Results on mass, radius, ionosphere, and atmosphere from Mariner 10 dual-frequency radio signals, Science, 185, 179, 1974.

Kennel, C. F., Magnetospheres of the planets, Space Sci. Rev., 14, 511, 1973.

McPherron, R. L., Substorm related changes in the geomagnetic tail: the growth phase, Planet. Space Sci., 20, 1521, 1972.

Meng, C.-I., and K. A. Anderson, J. Geophys. Res., 76, 873, 1971.

Murayama, T., Spatial distribution of energetic electrons in the geomagnetic tail, J. Geophys. Res., 71, 5547, 1966.

Ness, N. F., Y. C. Whang, and K. H. Schatten, Magnetic field observations near Mercury: preliminary results from Mariner 10, Science, 185, 151, 1974.

Ness, N.F., K.W. Behannon, R.P. Lepping, and Y.C. Whang, The magnetic field of Mercury: Part I, submitted to J. Geophys. Res., 1975.

Ogilive, K. W., J. D. Scudder, R. E. Hartle, G. L. Siscoe, H. S. Bridge, A. J. Lazarus, J. R. Asbridge, S. J. Bame, and C. M. Yeates, Observations at Mercury encounter by the plasma science experiment on Mariner 10, Science, 185, 145, 1974.

Simpson, J. A., J. H. Eraker, J. E. Lamport, and P. H. Walpole, Electrons and protons accelerated in Mercury's magnetic field, Science, 185, 160, 1974.

Siscoe, G. L., Particle and field environment of Uranus, submitted to Icarus, 1974.

Siscoe, G. L., and N. U. Crooker, A theoretical relation between Dst and the solar wind merging electric field, Geophys. Res. Let., 1, 11, 1974.

FIGURE CAPTIONS

Figure 1. Mariner 10 Mercury encounter trajectory in solar ecliptic coordinates. X-axis toward sun; Z-axis toward north ecliptic pole. Numbers refer to field and particle events identified in Figure 2 and discussed in text.

Figure 2. Combined plasma electron and magnetic field data covering two hours around Mariner 10 Mercury encounter. Data fields are magnetic field strength $\overline{F}$ (γ); solar ecliptic polar angles of the field orientation, ϕ(longitude measured east from Sun direction) and θ(latitude); electron count rate in the 389 ev channel, electron density, and electron thermal pressure. The 389 ev data field is representative of all channels measuring energies greater than ~ 100 ev. The density data field is representative of counts in all channels measuring energies less than ~ 100 ev.

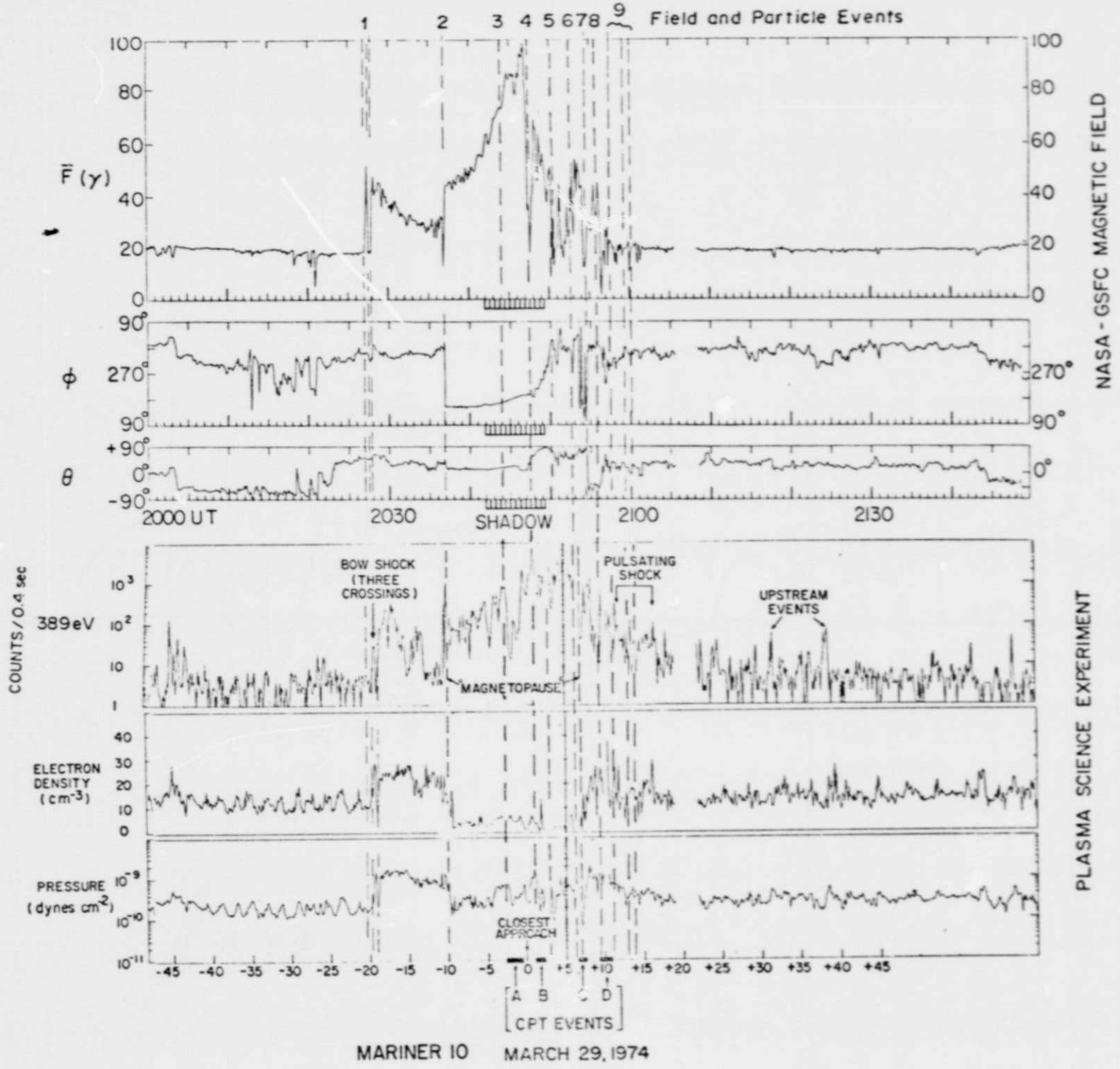
1 2 3 4 5 6 7 8 9 Field and Particle Events
$\bar{F}$ (γ)
100
80
60
40
20
0
φ
90°
270°
90°
θ
+90°
0°
-90°
2000 UT
2030
SHADOW
2100
2130
NASA - GSFC MAGNETIC FIELD
PLASMA SCIENCE EXPERIMENT
COUNTS / 0.4 sec
389eV
BOW SHOCK (THREE CROSSINGS)
MAGNETOPAUSE
PULSATING SHOCK
UPSTREAM EVENTS
ELECTRON DENSITY (cm⁻³)
PRESSURE (dynes cm⁻²)
CLOSEST APPROACH
-45 -40 -35 -30 -25 -20 -15 -10 -5 0 +5 +10 +15 +20 +25 +30 +35 +40 +45
A B C D
CPT EVENTS
MARINER 10 MARCH 29, 1974

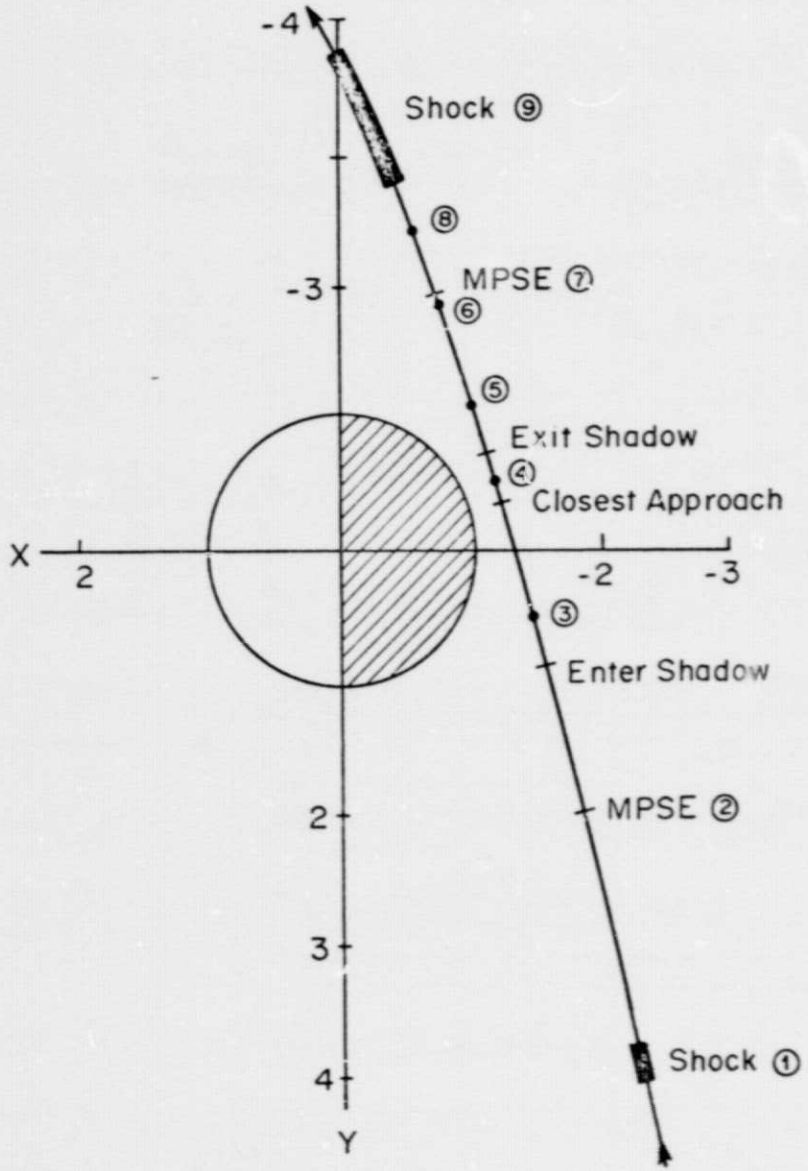
-4
Shock ⑨
⑧
-3
MPSE ⑦
⑥
⑤
Exit Shadow
④
Closest Approach
X
2
-2
-3
③
Enter Shadow
2
MPSE ②
3
Shock ①
4
Y

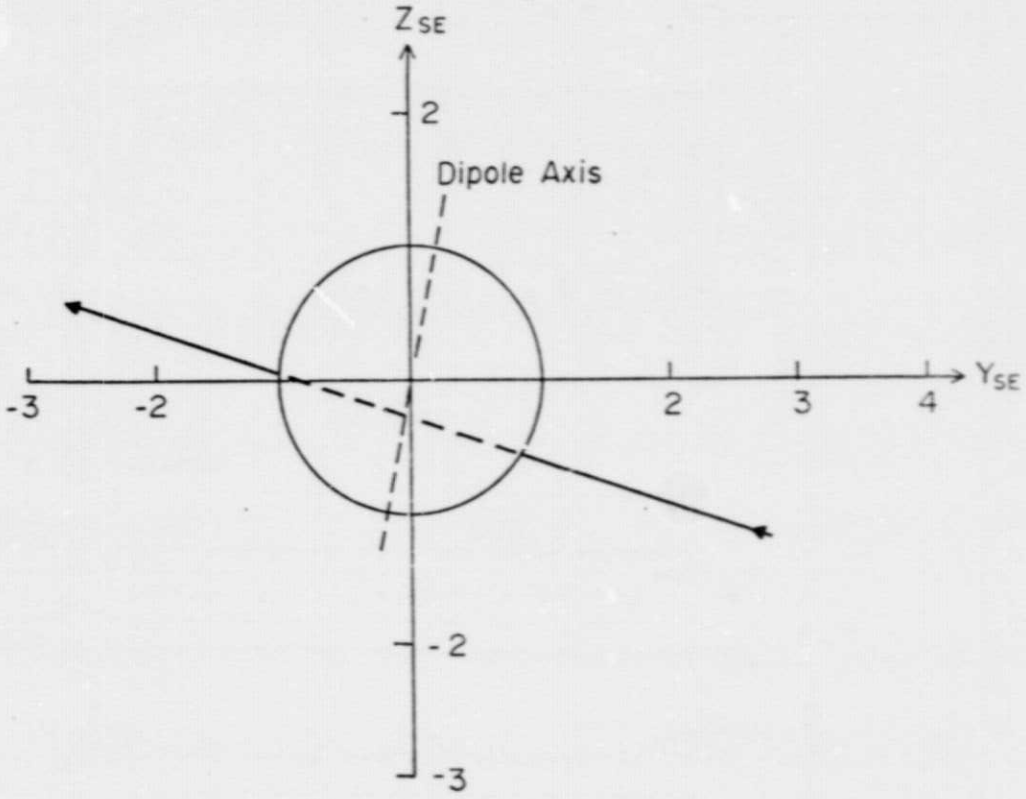
Z SE
2
Dipole Axis
-3
-2
2
3
4
Y SE
-2
-3